MGG

The vacuolar H^+-ATPase of *Saccharomyces cerevisiae* is required for efficient copper detoxification, mitochondrial function, and iron metabolism

David J. Eide[1], Jamie T. Bridgham[1], Zhong Zhao[1,*], James R. Mattoon[2]

[1] Department of Biochemistry and Molecular Biology, University of Minnesota-Duluth, Duluth, MN 55812-2487, USA
[2] Biotechnology Center University of Colorado, Colorado Springs, CO 80933-7150, USA

Received: ■■■

Abstract. Mutations in the *GEF2* gene of the yeast *Saccharomyces cerevisiae* have pleiotropic effects. The *gef2* mutants display a petite phenotype. These cells grow slowly on several different carbon sources utilized exclusively or primarily by respiration. This phenotype is suppressed by adding large amounts of iron to the growth medium. A defect in mitochondrial function may be the cause of the petite phenotype: the rate of oxygen consumption by intact *gef2* cells and by mitochondrial fractions isolated from *gef2* mutants was reduced 60%–75% relative to wild type. Cytochrome levels were unaffected in *gef2* mutants, indicating that heme accumulation is not significantly altered in these strains. The *gef2* mutants were also more sensitive than wild type to growth inhibition by several divalent cations including Cu. We found that the *cup5* mutation, causing Cu sensitivity, is allelic to *gef2* mutations. The *GEF2* gene was isolated, sequenced, and found to be identical to *VMA3*, the gene encoding the vacuolar H^+-ATPase proteolipid subunit. These genetic and biochemical analyses demonstrate that the vacuolar H^+-ATPase plays a previously unknown role in Cu detoxification, mitochondrial function, and iron metabolism.

Key words: Yeast – Vacuolar H^+-ATPase – Cu detoxification – Respiration – Iron metabolism

Introduction

The fungal vacuole is an acidic organelle that is analogous in many ways to the mammalian lysosome. The vacuole contains a variety of hydrolytic enzymes and plays an important role in the degradation of intracellular macromolecules. In addition, this organelle is involved in pH homeostasis and the compartmentalization of metabolites and ions (for review, see Klionsky et al. 1990). In this respect, the fungal vacuole is more similar to the vacuole of plant cells than it is to the mammalian lysosome. Many different cellular constituents are stored in the fungal vacuole, including amino acids, polysaccharides, and polyphosphates. The vacuole also plays an important role in the storage and homeostasis of metal ions (Gadd and White 1989). Vacuole-stored metal ions include such physiologically useful cations as Zn, Ca, and Mn as well as the nonphysiological cations Co, Pb, and Sr. Two reasons why metal cations are stored in the vacuole are: (1) the may be harmful to the cell when present in the cytoplasm at high concentrations and (2) their levels must be precisely controlled if they are to play a role in the regulation of cellular processes.

Vacuolar uptake of several cellular constituents is carried out by H^+/ion antiport systems, i.e. ion uptake into the vacuole is driven by proton efflux from the organelle. In vitro studies with purified vacuole vesicles have shown that H^+/ion antiport is the principal mechanism of vacuolar uptake of arginine, and the divalent cations Ca, Mg, Mn, and Zn (Ohsumi and Anraku 1983; Okorokov et al. 1985). The vacuole of *Saccharomyces cerevisiae* is maintained at a mildly acidic pH, approximately 6.2, while the cytoplasm is at neutral pH (Preston et al. 1989). This proton gradient is generated by an H^+-ATPase found in the vacuolar membrane and comprising as many as eight subunits (Kane et al. 1989). Subunits in the vacuolar H^+-ATPase complex are thought to be organized in a manner similar to the F_1F_0-ATPase of mitochondria (Bowman et al. 1986). Peripheral membrane proteins with catalytic activity are associated with a proton channel comprising integral membrane proteins. One of these integral membrane proteins is the 16 kDa proteolipid subunit encoded by the *VMA3* gene (Nelson and Nelson 1989; Ohya et al. 1986, 1991; Umemoto et al. 1990). This subunit binds N,N'-dicyclohexyl-carbodiimide (DCCD), an H^+-ATPase in-

Communicated by W. Gajewski

* *Present address:* Department of Biochemistry, University of Minnesota, Minneapolis, MN 55455, USA

Correspondence to: D. Eide, Department of Biochemistry and Molecular Biology, University of Minnesota-Duluth, 10 University Drive, Duluth, MN 558812-2487, USA

Ms. No. 317 Author Eide Ms. 41 Pages 10

Springer Prod.-Ges. Berlin / H. Stürtz AG, Würzburg
Provisorische Seitenzahlen / Provisional page numers 1. Korr. F Date 29.6.93

Table 1. Strains of *Saccharomyces cerevisiae*

Strain	Genotype	Source
JY102	*MATa ura3 leu2 lys2*	Greene et al. (1993)
JY140	*MATa ura3 leu2 lys2 gef2-1*	Greene et al. (1993)
JY146	*MATα ura3 leu2 his4 gef2-2*	Greene et al. (1993)
DBY2063	*MATa ura3 leu2*	D. Botstein
DBY2064	*MATα lys2 his4*	D. Botstein
DEY1121-6	*MATα ura3*	This work
DEY1121-10	*MATa lys2 ura3*	This work
DEY1121-20	*MATα his4*	This work
DEY1380	*MATα his4 gef2-1*	This work
K382-23A	*MATa ade2 can1 cyh2 his7 hom3 spo11 ura3*	YGSC[a]
DEY1378	*MATa ura3 leu2 lys2 gef2-1::pJB3 (GEF2 URA3)*	This work
JW557-1Dα	*MATα cup5*	Welch et al. (1989)
DEY1382	*MATα lys2 ura3 cup5*	This work
DEY1383	*MATa lys2 cup5*	This work
ΔVATc	*MATa ade2 his3 ura3 leu2 trp1 can1 vma3::LEU2*	Nelson and Nelson (1990)

[a] Yeast Genetics Stock Center, Berkeley, Calif.

hibitor that blocks proton translocation (Uchido et al. 1985).

Because of the many transport processes controlled by vacuolar pH, mutations that disrupt acidification are pleiotropic. For example, mutations in several vacuolar H^+-ATPase subunit genes cause cytosolic levels of Ca to be elevated (Ohya et al. 1991). Strains bearing these mutations were also found to be more sensitive than wild-type cells to the growth inhibitory effects of Zn and Cd as well as Ca (Ohya et al. 1986, 1991). Surprisingly, mutations in the vacuolar H^+-ATPase subunit genes caused cells to grow poorly on nonfermentable carbon sources (Ohya et al. 1986, 1991). In yeast, this phenotype, referred to as "petite", is usually associated with mutations that disrupt mitochondrial function.

In this report, we describe the characterization of three new alleles of the *VMA3* gene. Two of these alleles, *gef2-1* and *gef2-2*, were isolated because of their effects on growth on media containing nonfermentable carbon sources (Greene et al. 1993). The third allele, *cup5*, was isolated by Welch et al. (1989) because it conferred increased sensitivity to growth inhibition by Cu. Our analysis of these alleles indicates that the vacuolar H^+-ATPase plays an important role in Cu detoxification, mitochondrial function, and iron metabolism.

Materials and methods

Strains, media and genetic techniques. Strains used and their sources are described in Table 1. With the exception of K382-23A, JW557-1Dα, and ΔVATc, all strains were derived from the S288C strain of *S. cerevisiae*. DEY1380 is a haploid strain derived form a JY140 × DEY1121-20 diploid. DEY1378 was isolated by transforming JY140 with *Bam*HI-digested pJB3 (see subsequent section). DEY1382 and DEY1383 were derived from a JW557-1Dα × DEY1121-10 diploid. YPD (1% yeast extract, 2% peptone, 2% dextrose), YPGE (1% yeast extract, 2% peptone, 2% glycerol, 2% ethanol), SD media (0.67% yeast nitrogen base without amino acids, 2% dextrose, auxotrophy supplements as required) and techniques for the sporulation of diploids, the dissection of asci, and transformation of yeast spheroplasts were as described by Sherman et al. (1986). Genetic distances were calculated as described by Mortimer and Schild (1981). Cell number was monitored by measuring the optical density at 600 nm (OD_{600}); these values were converted to cell number with an empirically derived standard curve. Strain DH5α of *Escherichia coli* (Bethesda Research Laboratories, Bethesda, Md.) was used for molecular cloning experiments.

DNA manipulations. DNA fragment isolations, ligations, and *E. coli* transformations were performed essentially as described by Sambrook et al. (1989). The wild-type *GEF2/VMA3* gene was isolated from a plasmid library constructed from partially digested *Sau*3A genomic fragments cloned into the *Bam*HI site of YEp24 (Carlson and Botstein 1982). The plasmid pZZ5 was isolated from approximately 10 000 independent plasmid transformants because of its ability to complement the growth defect of a *gef2-1* strain (JY140) on YPGE. Transformed cells were collected, pooled, and replated to YPGE. A single transformant capable of efficient growth on this medium was isolated, and plasmid DNA was purified from it and amplified in *E. coli*. This plasmid was then transformed into yeast strains JY140 and JY146 to test for complementation of the *gef2-1* and *gef2-2* alleles, respectively. Plasmids pJB1, pJB2, pJB5, pJB6, and pJB7 (Fig. 3) are derivatives of pZZ5 and were constructed as follows. pJB1 was constructed by digesting pZZ5 with *Kpn*I, isolating the vector-containing fragment, and religating with DNA ligase. Plasmids pJB2, pJB5, and pJB6 were constructed by inserting the 6 kb *Pst*I-*Sal*I, 2.7 kb *Hin*dIII-*Sal*I, and 3.6 kb *Sac*I-*Xba*I fragments from pZZ5, respectively, into YEp352 (Hill et al. 1986) that had been digested with the same restriction endonucleases as the fragment. pJB7 was constructed by inserting a 2.2 kb *Hin*dIII-*Hin*dIII fragment from pJB2 into YEp352. One of the two *Hin*dIII sites utilized in this subcloning was present in the multiple cloning site of the

vector in pJB2; the subcloned fragment corresponds to the *Pst*I-*Hin*dIII fragment of pZZ5. pJB3 was constructed by inserting the entire 12 kb *Sal*I-*Sma*I fragment from pZZ5 into *Sal*I + *Sma*I-digested YIp352 (Hill et al. 1986). Plasmid pJB3 was digested with *Bam*HI, which cuts within the insert, and transformed into a haploid *ura3 gef2-1* strain (JY 140). This method directs integration of the plasmid to the genomic location of the cloned DNA (Rothstein 1991). All DNA sequencing was performed by the chain-termination method (Sequenase Version 2.0, United States Biochemical, Cleveland, Ohio) modified as described by Borson et al. (1992). The *VMA3/GEF2* gene-containing insert in pJB6 was sequenced using a series of nested deletions produced by the combined action of exonuclease III and nuclease S1 (Erase-a-Base, Promega, Madison, Wis.) (Henikoff 1984) and an oligonucleotide primer (5′-CGACGGCCAGTGCCAAGC-3′) derived from sequences adjacent to the multiple cloning site of YEp352. DNA for sequencing the *gef2-1*, *gef2-2*, and *cup5* mutant alleles was obtained by polymerase chain reaction (PCR) amplification (AmpliTaq, Perkin Elmer Cetus, Norwalk, Conn.) from genomic DNA isolated from strains JY140, JY146, and JW557-1Dα, respectively. Oligonucleotide primers flanking the *VMA3* protein coding region used for this amplification corresponded to sequences 5′-GAGAAGATCGTGTTTATTGC-3′ (positions 151–170) and 5′-GTATACTCTATTCCTGCTTTAG-3′ (positions 743–722) based on the numbering system of Nelson and Nelson (1989). Direct sequencing of the resulting PCR products was performed using the PCR primers and one additional primer derived from sequences within the protein coding region, i.e. 5′-CCTGTTATTATGGCTGG-3′ (positions 388–404).

Quinacrine staining of yeast vacuoles. In vivo quinacrine staining of yeast vacuoles was performed essentially as described by Roberts et al. (1991). Cells were grown to exponential phase in YPD medium, collected by centrifugation for 5 min at 1000 *g*, and resuspended at a cell density of 1×10^7 cells/ml in YPD buffered to pH 7.6 with 50 mM $NaPO_4$. A 500 µl aliquot of cells was transferred to a 1.5 ml microfuge tube and quinacrine was added to a final concentration of 200 µM from a 20 mM stock prepared in distilled water. The cells were incubated at 30° C for 20 min with occasional shaking. Cells were harvested by centrifuging 5 s in a microfuge at 12 000 *g*, washed once in SD medium prepared without glucose and buffered to pH 7.6 with 50 mM $NaPO_4$, and resuspended in 500 µl of the wash buffer. Cells were transferred to concanavalin A-treated microscope slides and viewed in a Leitz Orthoplan fluorescence microscope at an excitation wavelength of 490 nm and an emission wavelength of 525 nm.

Determination of O_2 consumption rates in intact cells. The rate of O_2 consumption by intact cells was determined using the Standard System from Yellow Springs Instrument Co, Yellow Springs, Ohio, which includes an oxygen electrode (Model 5331), standard bath assembly (Model 5301), and biological oxygen monitor (Model 5300). Cells were grown to exponential phase in YPGE medium, collected by centrifugation for 5 min at 1000 *g* at 4° C, and resuspended at 1/50th of the original volume in chilled YPGE medium. The cells were assayed in 3 ml of YPGE medium preequilibrated to 30° C. After the electrode was inserted into the reaction vessel, $2.0–4.0 \times 10^7$ cells were added in a 50 µl volume, and the decrease in $\%O_2$ was recorded. The O_2 consumption rate of the cells was calculated from the slope of the line of $\%O_2$ consumed per minute. Percent O_2 was converted to nanomoles O_2 using a value of 0.223 mM as the equilibrium (100%) concentration of dissolved O_2 in an aqueous solution at 30° C (Chappell 1964).

Preparation and analysis of isolated mitochondrial fractions. Cells were grown with aeration for 16–24 h in 700 ml YPGE in 2 l flasks at 30° C. At a density of $2.0–4.0 \times 10^7$ cells/ml, the cells were harvested and mitochondrial fractions prepared as described by Yaffe (1991). Protein concentrations were determined by the method of Bradford (1976; BioRad Laboratories, Richmond, Calif.). O_2 consumption rates of mitochondrial fractions were determined using the method of Yaffe (1991) with the Standard System oxygen monitor at 30° C. Mitochondrial fractions were added to 3 ml assay buffer (0.6 M mannitol, 20 mM HEPES-KOH, 10 mM KPO_4, 2 mM $MgCl_2$, 1 mM EDTA, 5 mg/ml bovine serum albumin, pH 7.4) to a final concentration of 250–500 µg/ml protein. Respiration rate was measured for 1–2 min and 0.5 M TRIS-succinate, pH 7.4 was added to a final concentration of 10 mM. Respiration rate (state 4 respiration) was then measured for another 1–2 min. ADP was added to a final concentration of 200 µM from a 20 mM stock, and respiration was measured (state 3 respiration). The respiratory control ratio, i.e. the state 3 respiration rate divided by the state 4 respiration rate, for all samples, ranged from 2.0–2.6, indicating that O_2 consumption and oxidative phosphorylation were coupled. The O_2 consumption rate for state 3 respiration was calculated from the slope of the line of $\%O_2$ consumed per minute and converted to nanomoles O_2 using the conversion factor given in the previous section. Citrate synthase activity in mitochondrial fractions was measured by the method of Parvin (1969). Mitochondrial fractions were diluted tenfold (to 0.2–1.0 mg/ml protein) into 50 mM $NaPO_4$, 1% Triton X-100, 1 mM EDTA, pH 7.4. Aliquots (10 µl) of the diluted mitochondrial fractions were assayed in 0.1 M TRIS-HCl, 0.25 mM 5,5′-dithiobis-(2-nitrobenzoic acid) (DTNB), 0.2 mM oxaloacetic acid, 0.1 mM acetyl-CoA, pH 8.0 at 415 nm. Units are defined as micromoles CoASH generated per minute and were calculated using a molar absorbance coefficient of 13 600 for DTNB mercaptide ion.

Determination of whole-cell cytochrome spectra. Cells were grown to stationary phase in YPD, reinoculated into YPGE and grown with aeration for four to five doublings at 30° C. Cells were harvested and whole-cell spectra were determined with a double beam spectrophotometer using yeast suspensions containing 25 mg/ml dry weight. Whole milk diluted to 20% was used as a

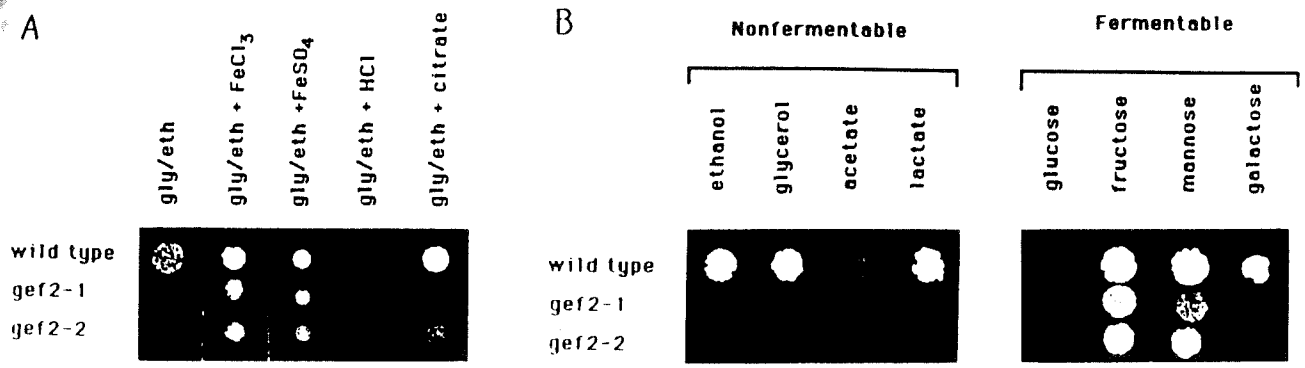

Fig. 1A, B. Growth phenotypes of *gef2* strains. Wild-type (JY102), *gef2-1* (JY140), and *gef2-2* (JY146) cells were grown to stationary phase in YPD medium, diluted, and approximately 200 cells in a 5 µl volume were spotted onto plates containing **A** YPGE, YPGE plus 5 mM $FeCl_3$, YPGE plus 5mM $FeSO_4$, and YPGE to which the pH has been adjusted to 5.0 with HCl or with 20 mM citrate, and **B** YP medium containing the nonfermentable carbon sources glycerol, ethanol, acetate, and lactate and the fermentable carbon sources glucose, fructose, mannose, and galactose. All carbon sources were supplied at an initial concentration of 2%. The plates were then incubated at 30° C for 3 days

reference. Cytochromes were reduced by adding a few milligrams of dithionite to the sample cuvette.

Results

Isolation of mutations in the GEF2 *gene*

The studies described in this paper were initiated to identify genes involved in iron metabolism in *S. cerevisiae*. We reasoned that yeast strains defective in iron metabolism would grow poorly on nonfermentable carbon sources unless the medium was supplemented with iron. This hypothesis was the basis for the development of a genetic screen, described in detail elsewhere (Greene et al. 1993), carried out to identify mutants defective for iron metabolism. From ~10 000 ethyl methanesulfonate (EMS)-mutagenized cells plated on a rich medium containing glycerol and ethanol (YPGE) as carbon sources, 3 strains were identified that grew poorly unless supplemented with 5 mM $FeCl_3$.[1] This phenotype was named "Gef$^-$" for *g*lycerol/*e*thanol, *Fe*-requiring. Genetic analysis indicated that these three strains each contained a single, recessive, nuclear mutation responsible for the Gef$^-$ phenotype. The Gef$^-$ mutations were assigned by complementation testing into two groups, *GEF1* and *GEF2*. One allele belonged to the *GEF1* complementation group (*gef1-1*) and two alleles corresponded to the *GEF2* complementation group (*gef2-1* and *gef2-2*). The *GEF1* gene encodes a potential integral membrane protein with sequence similarity to chloride channel proteins (Greene et al. 1993). We report here that the *GEF2* gene is identical to the *VMA3* gene and encodes the proteolipid subunit of the vacuolar H^+-ATPase (Nelson and Nelson 1989; Umemoto et al. 1990).

[1] While $FeCl_3$ is not completely soluble in the growth medium at this concentration, we refer to 5 mM as the nominal concentration of $FeCl_3$

To verify that the growth enhancement effect of $FeCl_3$ on *gef2-1* and *gef2-2* cells depended on iron per se, we tested the growth of these cells on YPGE media with various supplements. Mutant *gef2-1* and *gef2-2* cells grew at wild-type rate on YPGE medium supplemented with either 5 mM $FeCl_3$ or $FeSO_4$ (Fig. 1A), indicating that the growth response did not depend on the particular iron salt used. Because these iron supplements substantially lower the pH of the YPGE medium, i.e. from 6.5 to 5.0, it was unclear whether the *gef2-1* and *gef2-2* mutants were responding to the increased iron concentration or the lowered pH. To distinguish between these two possibilities, we tested the ability of wild-type and mutant cells to grow on YPGE in which the pH had been lowered to 5.0 with HCl or buffered to pH 5.0 with 20 mM citrate. Although some improvement in growth was observed with lowered pH, neither modification enhanced the ability of *gef2-1* and *gef2-2* cells to grow on YPGE to as great an extent as $FeCl_3$ or $FeSO_4$ (Fig. 1A). Therefore, the growth-enhancing property of iron supplements was dependent largely on iron and not simply on changes in pH.

To determine whether the poor growth observed for *gef2-1* and *gef2-2* cells on glycerol/ethanol-containing media is also observed on other carbon sources, we plated wild-type, *gef2-1*, and *gef2-2* cells on rich media, each supplemented with one of several carbon sources. These included the nonfermentable carbon sources acetate and lactate and the fermentable carbon sources glucose, fructose, mannose, and galactose. Mutant *gef2-1* and *gef2-2* cells grew poorly on all nonfermentable carbon sources (Fig. 1B). For all of these compounds, almost wild-type growth rates were restored to the *gef2-1* and *gef2-2* strains by addition of 5 mM $FeCl_3$ (data not shown). The *gef2-1* and *gef2-2* mutants grew at near wild-type rates on all fermentable carbon sources except galactose. As with the nonfermentable carbon sources, the growth defect on galactose was suppressed by adding 5 mM $FeCl_3$ (data not shown). Galactose differs from the other fermentable carbon sources used here in that approximately 90% of the ATP derived from

Table 2. Genetic mapping of *gef2-1*

Gene pair	PD	NPD	TT	Total	Map distance (cM)
can1/gef2	9	0	17	26	32
ura3/gef2	24	0	6	30	10
can1/ura3	9	0	21	30	35

The haploid strains DEY1380 (*gef2-1*) and K382-23A (*ura3 can1*) were crossed to generate a multiply heterozygous diploid. This diploid was sporulated and the segregation of the *can1*, *gef2*, and *ura3* mutations was scored. The number of parental ditype (PD), nonparental ditype (NPD), tetratype (TT), and total tetrads scored, and the map distances in centimorgans calculated from these data are shown

galactose under aerobic conditions is generated by respiration (Lagunas 1986). These results indicated that *gef2-1* and *gef2-2* mutants are not simply defective for uptake of a given carbon source. Rather, *gef2-1* and *gef2-2* cause a petite phenotype, i.e. poor growth on all carbon sources utilized exclusively or primarily by respiration.

GEF2 *is identical to the* VMA3 *gene*

Genetic mapping of the *gef2-1* allele first suggested a relationship between *GEF2* and *VMA3*, which encodes the 16 kDa proteolipid subunit of the vacuolar H^+-ATPase. Chromosome blotting mapped the *GEF2* gene to chromosome V (Carle and Olson 1985) (data not shown). To map the gene more precisely, a *gef2-1* haploid strain (DEY1380) and a *ura3 can1* haploid (K382-23A) were crossed to yield a diploid strain heterozygous for the *gef2*, *ura3*, and *can1* alleles. Tetrads were dissected and haploid segregants were isolated, genotyped, and map distances were calculated (Table 2). These results demonstrated that the *GEF2* gene is located between the *URA3* and *CAN1* genes. This site is within 2 cM of the position of the previously mapped *VMA3* gene (Ohya et al. 1986).

Mutations that disrupt the *VMA3* gene prevent vacuolar acidification. Acidified vacuoles of wild-type cells accumulate the weak base quinacrine whereas vacuoles in *vma3* mutant strains fail to accumulate this dye (Nelson and Nelson 1990). We tested whether *gef2-2* was allelic to *VMA3* by assessing the ability of mutant cells to accumulate quinacrine in their vacuoles. Figure 2 shows that the vacuoles of *gef2-2* mutant cells stained poorly with quinacrine and provides evidence that vacuolar acidification is defective in these cells.

Analysis of the cloned *GEF2* gene verified that *GEF2* and *VMA3* represent the same gene. The wild-type *GEF2* gene was cloned by complementation of the growth defective phenotype of a *gef2-1* strain on YPGE. A *gef2-1* mutant strain (JY140) was transformed with a genomic library constructed in a yeast episomal plasmid vector. One plasmid, pZZ5, was isolated that complemented the *gef2-1* allele; subsequent analysis demonstrated that this plasmid also complemented the *gef2-2* mutation. Plasmid pZZ5 contains an insert of approximately 12 kb;

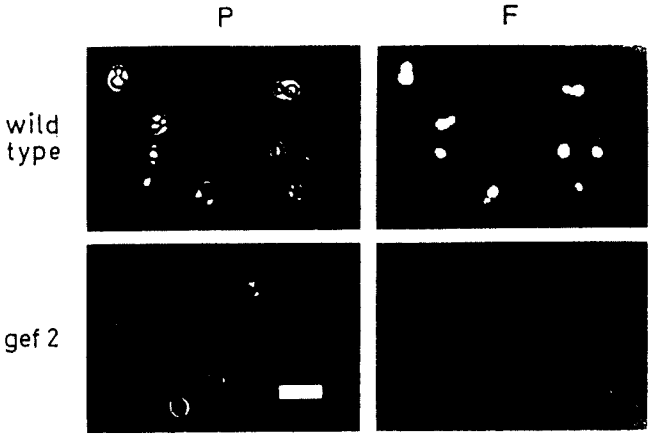

Fig. 2. Mutant *gef2-2* cells are defective for vacuolar acidification in vivo. Wild-type (JY102) and *gef2-2* (JY146) cells were grown to exponential phase in YPD, collected, and stained with quinacrine. The cells were then washed, mounted, and viewed by phase contrast microscopy (*P*) and fluorescence microscopy using standard fluorescein fluorescence wavelengths (*F*). Bar represents 50 μm

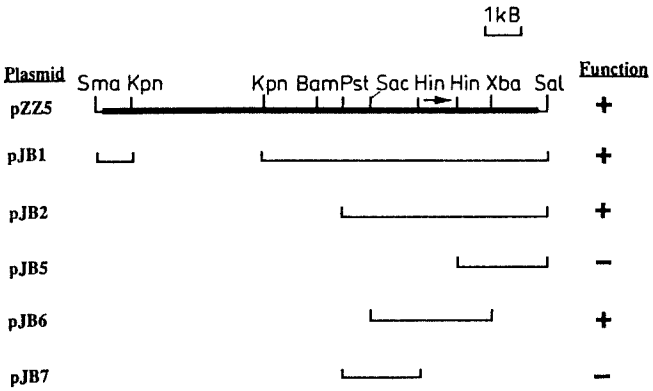

Fig. 3. Partial restriction map of the yeast genomic insert in pZZ5 and its derivatives. The plasmid pZZ5 was digested with the restriction enzymes *Bam*HI (Bam), *Hin*dIII (Hin), *Kpn*I (Kpn), *Pst*I (Pst), *Sac*I (Sac), *Sal*I (Sal), *Sma*I (Sma), and *Xba*I (Xba). The map shows the position of restriction sites within the cloned insert *(thick line)* and flanking vector DNA *(thin line)*. Only sites within the insert that are relevant to the discussion are included. The *lines* below the map indicate the fragments that are present in the subclones. The five derivative plasmids were tested for their ability to complement the YPGE growth defect of a *gef2-1* haploid strain (JY140) and the results are indicated as (+) for successful complementation and (−) for failure to complement. The *arrow* indicates the site of the *VMA3* open reading frame and the direction of transcription

a partial restriction map of this fragment is shown in Fig. 3.

We used a test of genetic linkage to demonstrate that the cloned DNA fragment in pZZ5 contains the *GEF2* gene as defined by the *gef2-1* and *gef2-2* alleles. The insert fragment was subcloned into a yeast integrating plasmid, a vector that contains no yeast replication origin and that can be propagated in a yeast strain only by integration of the plasmid into a chromosomal site. Digestion of the resulting plasmid, pJB3, with a restriction endonuclease that cuts at a single site within the cloned insert directs integration of the plasmid by homologous

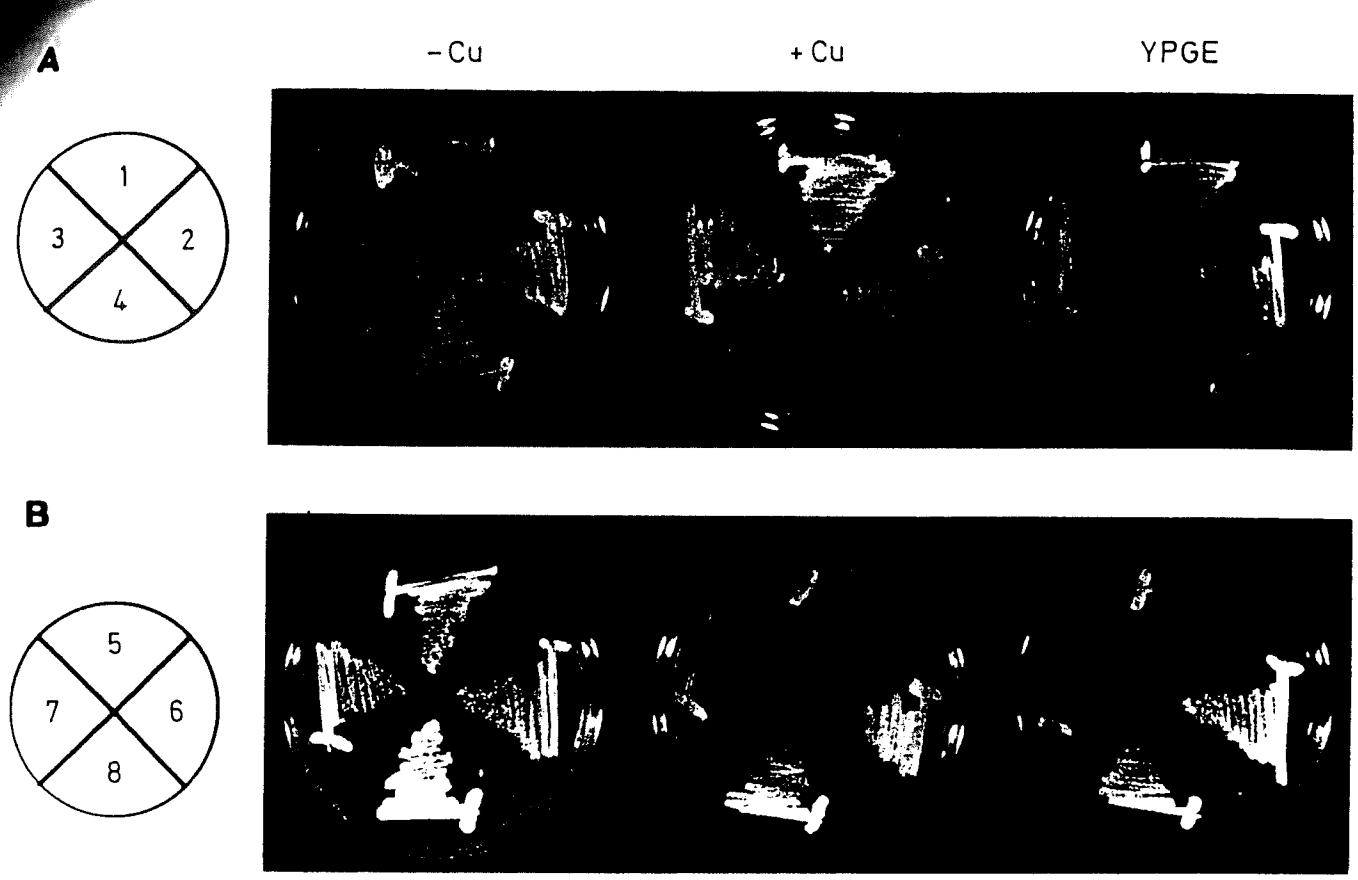

Fig. 4A, B. Genetic evidence that *cup5* is allelic to *VMA3*. **A** Haploid wild-type, *gef2-2* (JY146), and *cup5* (DEY1383) strains were each crossed to a wild-type strain or to each other. The resulting diploids were inoculated onto an SD agar plate plus 0.75 mM Cu and a YPGE plate and grown for 3 days at 30° C. Diploids shown are wild type × wild type (1), *cup5* × wild type (2), *gef2-2* × wild type (3), and *cup5* × *gef2-2* (4). **B** Haploid *gef2-2* (JY146) and *cup5* (DEY1382) strains were transformed with either YEp352 or pJB6. Transformants were isolated, inoculated onto a SD agar plate plus 0.75 mM Cu and a YPGE plate and grown for 3 days at 30° C. Transformants shown are *gef2-2* (YEp352) (5), *gef2-2* (pJB6) (6), *cup5* (YEp352) (7), and *cup5* (pJB6) (8)

recombination to the genomic site of the insert. The pJB3 plasmid was linearized and transformed into a *gef2-1* haploid strain (JY140). The transformants isolated showed no Gef$^-$ phenotype indicating that the plasmid complemented in single copy and that the isolated fragment does not contain an extragenic multicopy suppressor.

The resulting strain was crossed with a wild-type strain (DEY1121-20) and a *gef2-2* strain (JY146). Tetrads from these diploid strains were dissected and analyzed for the segregation of Ura$^-$ and Gef$^-$ phenotypes. Among the haploid segregants of 16 tetrads dissected from the cross with the *gef2-2* mutant, the Gef$^-$ and Ura$^-$ phenotypes each segregated 2:2. All of the Gef$^+$ segregants from this diploid were Ura$^+$. This segregation pattern indicated that a single insertion in the genome occurred during transformation. In the cross with the wild-type haploid, 19 tetrads were dissected and all segregated 4:0 Gef$^+$:Gef$^-$. This result showed that the insertion site of pJB3, as directed by homologous recombination of the cloned fragment at its chromosomal locus, is tightly linked, i.e. within 2.6 cM (i.e. < 10 kb) (Mortimer and Schild 1981), to the *gef2-1* mutation. These data support the assertion that pZZ5 contains the wild-type *GEF2* gene.

To determine the location of the *GEF2* gene within the cloned insert of pZZ5, we performed deletion analysis. Deletions were constructed within pZZ5 or smaller fragments from the pZZ5 insert were subcloned into the yeast episomal vector YEp352 (Hill et al. 1986). These derivative plasmids were then tested for their ability to complement a *gef2-1* mutation. The results indicated that the 3.4 kb *Xba*I-*Sac*I fragment retained complementing activity (Fig. 3). We sequenced this fragment and identified a long open reading frame (ORF) that would potentially encode a product of 160 amino acids with a predicted molecular mass of 16 kDa. Comparison of the amino acid sequence of this ORF with sequences in the Swiss-Prot database (Version 23) indicated that this gene was highly similar to a group of genes encoding the proteolipid subunit of the vacuolar H^+-ATPase from several organisms. A subsequent literature search revealed that the *S. cerevisiae* gene that encodes this protein, referred to in separate reports as *CLS7* (Ohya et al. 1986), "VATPc" (Nelson and Nelson 1990), and *VMA3* (Umemoto et al. 1990), had also been sequenced.

CUP5 is identical to the VMA3 *gene*

Mutations in the genes encoding the vacuolar H^+-ATPase subunits cause a phenotype in which mutant cells are more sensitive than wild-type cells to the growth inhibitory effects of several divalent cations, including Ca, Mn, and Zn (Ohya et al. 1986, 1991, see below). We noted with interest that a mutation causing hypersensitivity to growth inhibition by Cu, *cup5*, had been mapped to within 2-3 cM of the *GEF2/VMA3* locus (Welch et al. 1989). This coincidence suggested that *cup5* might also be a mutant allele of the *VMA3* gene. We found that a *cup5* strain was defective for vacuolar acidification as judged by in vivo staining with quinacrine (data not shown). Two genetic tests were used to demonstrate that *CUP5* and *VMA3* are identical. First, *cup5* and *gef2-2* failed to complement each other for Cu sensitivity or growth on respired carbon sources (Fig. 4A). Second, the smallest of the *GEF–2*-complementing plasmids we generated, pJB6 (Fig. 3), complemented the *cup5* mutation for both phenotypic defects (Fig. 4B). These results indicated that *CUP5* is the same gene as *GEF2/VMA3* and that mutations in this gene cause increased sensitivity to growth inhibition by Cu.

DNA sequence analysis of vma3 *mutations*

The final proof that the *gef2* and *cup5* alleles were the result of mutations in the *VMA3* gene was obtained by DNA sequence analysis. The *VMA3* mutant alleles *gef2-1*, *gef2-2*, and *cup5* as well as their wild-type parental alleles were sequenced. The *VMA3* sequences from the wild-type strains corresponding to the genetic backgrounds of both the *gef2* and *cup5* strains were found to be identical to one another and to the published sequence (Nelson and Nelson 1989). In the sequence of the *VMA3* genes from the three mutant strains, a single base substitution was detected within the coding region of *VMA3* (Table 3). Each base substitution was the result of a transition mutation, i.e. C to T or A to G. Each single base substitution causes a single amino acid substitution (Table 3). Three different sites are altered in the predicted amino acid sequence: amino acids 10 (*gef2-1*), 112 (*cup5*), and 147 (*gef2-2*).

Effect of vma3 *mutations on sensitivity to growth inhibition by divalent cations*

It has previously been reported that mutations disrupting vacuolar H^+-ATPase function increase sensitivity to the toxic effects of Ca, Mn, and Zn (Ohya et al. 1986, 1991). As we have shown, *vma3* mutations also increase sensitivity to Cu toxicity (Fig. 4). The resistance of *vma3* mutants to any of these cations has not been assessed quantitatively and the relative importance of the vacuolar H^+-ATPase in controlling their toxicity was unknown. We determined the effects of the *gef2* and *cup5* alleles on cation sensitivity by assessing the resistance of strains bearing these alleles to a range of concentrations of these divalent cations. A strain, ΔVATc, bearing a disruption allele in which the *LEU2* gene was inserted into the *VMA3* coding region was included in this analysis (Nelson and Nelson 1990). Haploid strains were tested for growth on agar plates containing a series, in two-fold increments, of concentrations of Cu, Ca, Mn, or Zn. The maximum levels of each cation in which the strains could grow are listed in Table 4. All *vma3* mutations increased sensitivity to the toxic effects of these cations. In general, the ΔVATc allele was the most sensitive of the alleles tested. In this strain, the maximum tolerable level of each cation decreased 5- to 40-fold. The *gef2-1* allele was the least severely affected, retaining normal sensitivity to Ca and better resistance than the other mutant alleles to Mn and Zn. These observations suggest that the *gef2-1* allele retains partial function.

Table 3. Sequence alterations in *vma3* mutant alleles

Strain	Codon	Wild type		Mutant	
		sequence	amino acid	sequence	amino acid
gef2-1	10	CCT	Pro	C*T*T	Leu
gef2-2	147	GCT	Ala	G*T*T	Val
cup5	112	GGT	Gly	G*A*T	Asp

Table 4. Effect of *vma3* mutations on sensitivity to divalent cations

Strain	Maximum tolerable level (mM)			
	Cu	Ca	Mn	Zn
Wild type	1.0	> 100	5.0	5.0
gef2-1	0.25	> 100	1.0	1.0
gef2-2	0.5	10	0.5	0.1
cup5	0.5	10	0.5	0.25
ΔVATc	0.1	5	1.0	0.25

Wild type (JY102), *gef2-1*, (JY140), *gef2-2* (JY146), *cup5* (JW557-1Dα), and ΔVATc were grown to stationary phase on YPD, diluted, and approximately 10^4 cells were inoculated in a 5 μl volume to YPD plates (for Ca, Mn, and Zn) or SD plates (for Cu) containing varying concentrations of divalent cations provided as the chloride salts. These plates were incubated for 3 days at 30° C and scored for the ability of the inoculated cells to form a colony. Isogenic parents of *cup5* (X2180-1A) and ΔVATc (W303) were also tested and found to be equivalent in sensitivity to JY102

Effects of vma3 *mutations on mitochondrial function*

All *vma3* mutants analyzed in this study share the phenotype of poor growth on media containing carbon sources utilized by respiration. We examined this apparent respiration defect with intact YPGE-grown cells and with isolated mitochondria from YPGE-grown cells (Table 5). It should be noted that *vma3* mutants do grow, albeit very slowly, on YPGE. Severe respiratory defects were detected in *gef2-1* and *gef2-2* strains. Intact *gef2-1* and *gef2-2* cells showed only 30%–40% the wild-type rate of O_2 consumption on glycerol and ethanol as substrates. Furthermore, we found that isolated mitochondria from

Table 5. Effect of *gef2* mutations on O_2 consumption and mitochondrial function

Strain	O_2 consumption rate		Citrate synthase activity[c]
	intact cells[a]	mitochondrial fractions[b]	
Wild type	2.2 ± 0.2	0.35 ± 0.04	4.2 ± 0.7
gef2-1	0.7 ± 0.1	0.09 ± 0.01	5.0 ± 0.2
gef2-2	0.9 ± 0.1	0.10 ± 0.01	3.4 ± 0.6

Wild type (JY102), *gef2-1* (JY140), and *gef2-2* (JY146) cells were inoculated into YPGE and grown to exponential phase. Cells were then harvested and assayed for O_2 consumption rate in fresh YPGE at 30° C. Mitochondrial fractions were isolated from each culture and assayed for O_2 consumption rate (state 3 respiration) using succinate as substrate at 30° C. Citrate synthase assays were performed on the isolated mitochondrial fractions at 25° C. Units are equal to micromoles per minute CoASH generated. Values are the mean of at least two separate experiments each performed in duplicate ± one standard deviation

[a] Nanomoles O_2 per minute per 10^6 cells

[b] Micromoles O_2 per minute per milligram protein

[c] Units per milligram protein

gef2-1 and *gef2-2* cells consumed O_2 at approximately 25% of the wild-type rate. Citrate synthase levels, however, were similar to wild type in the mutant-derived mitochondria, indicating that the *vma3* respiration defect was not caused by a general disruption in mitochondrial enzyme activities.

The respiration defect of *vma3* mutants is suppressed by the addition of high levels of iron to the growth medium (Fig. 1A). This observation suggested that mitochondrial dysfunction in these mutants could result from a mitochondrial iron deficiency. Such a deficiency may be detectable as a reduction in cytochrome accumulation. Whole-cell spectral analysis of cytochrome levels in YPGE-grown cells bearing the *vma3* alleles *gef2-1* and *gef2-2* did not detect any alteration in the levels of cytochromes *a*, *b*, and *c* when compared with wild-type cells (data not shown). Furthermore, no increased accumulation of Zn-protoporphyrin was observed in the mutants. Therefore, the respiratory defect of mitochondria in *vma3* cells is not caused by major perturbations in cytochrome accumulation.

Discussion

Our results demonstrate for the first time that the yeast vacuolar H^+-ATPase plays an important role in Cu detoxification. The mechanism of Cu detoxification in *S. cerevisiae* has been studied extensively and attributed almost solely to metallothionein, a cytoplasmic Cu-binding protein encoded by the *CUP1* gene. Strains bearing a mutation in which the *CUP1* gene was deleted, the *cup1*$^{\Delta}$ allele, grew poorly when 5 μM $CuCl_2$ was present in the medium whereas an isogenic wild-type strain showed a similar degree of sensitivity to 25 μM $CuCl_2$ (Ecker et al. 1986). Mutations in the *VMA3* gene, encoding the H^+-ATPase proteolipid subunit, reduce by as much as tenfold the level of Cu in which yeast cells can grow. This observation indicates that the vacuole plays a role in Cu detoxification of equal importance to that of metallothionein. We cannot say at this time whether the *vma3* mutations disrupt some aspect of the metallothionein-dependent mechanism of Cu detoxification or if some other, independent mechanism is altered.

The vacuolar H^+-ATPase is also clearly important for the detoxification of Ca, Mn, and Zn. The *vma3* mutations described in this report caused 10- to 50-fold reductions in the tolerable levels of these cations. The mechanism of toxicity of these metals is poorly understood. Numerous studies indicate that Ca plays an important role as a secondary messenger in the control of cell division (for review, see Anraku et al. 1991). Genetic analysis of *CMD1* (Ohya and Anraku 1989), the gene encoding the ubiquitous Ca-binding protein calmodulin, and of *PKC1* (Levin et al. 1990), the gene encoding the Ca-dependent enzyme protein kinase C, has demonstrated the importance of these proteins and intracellular Ca in cell cycle regulation. The toxic effects of Ca in *vma3* mutants may be due to aberrant regulation of the processes controlled by these proteins. Cu toxicity, on the other hand, may result from the ability of this metal to generate reactive oxygen radials such as hydroxyl radical, OH, which can then cause oxidative damage to the cell (Halliwell and Gutteridge 1992).

One hypothesis to explain the pleiotropic effects of mutations in the *VMA3* gene on cation sensitivity is that Ca, Cu, Mn, and Zn are each taken up and sequestered in the vacuole; this compartmentalization limits their toxicity. Uptake of these metals into the vacuole from the cytoplasm may require an H^+/ion antiport transport system. Evidence from in vitro analysis of cation uptake by vacuolar membrane vesicles indicates the presence of H^+/ion antiporters in the vacuole membrane for the uptake of Ca, Mn, and Zn (Ohsumi and Anraku 1983; Okorokov et al. 1985). A similar system may also be present for Cu uptake into the vacuole although such a mechanism has not yet been demonstrated. Mutations in vacuolar H^+-ATPase subunit genes that raise the pH of the vacuole would then be defective for sequestering these metals in the vacuole. This hypothesis predicts that mutations in the genes encoding the subunits of the vacuolar H^+-ATPase should be associated with higher cytoplasmic levels of these metals; this has been demonstrated for Ca (Ohya et al. 1991).

If an acidic vacuolar pH provides the driving force for the accumulation of Ca, Cu, Mn, and Zn in the vacuole, all mutations that disrupt the function of an H^+-ATPase subunit should result in increased sensitivity to these cations. Increased sensitivity to Ca, Mn, and Zn was observed for mutations in the genes *TFP1/VMA1*, *VMA11*, *VMA12*, and *VMA13*, all of which are required for vacuolar H^+-ATPase activity (Ohya et al. 1986, 1991). We found that a mutation *(tfp1-Δ8)* (Shih et al. 1988) in one of these genes, *TFP1/VMA1*, also increased sensitivity to Cu (D. Eide, unpublished observations). Therefore, Cu hypersensitivity may be a phenotype shared by mutations in many genes required for vacuolar acidification. Welch et al. (1989) isolated mutations in two other genes, *CUP3* and *CUP14*, that caused the same

degree of sensitivity to Cu as the *cup5* mutation. These genes may encode other subunits of the vacuolar H^+-ATPase or other proteins that are required for vacuolar acidification.

In addition to cation hypersensitivity, another phenotype shared by several mutants defective in their vacuolar H^+-ATPase is that they grow slowly on nonfermentable carbon sources. Anraku and coworkers reported that strains bearing mutations in the genes *TFP1/VMA1, VMA2, VMA3, VMA11, VMA12,* and *VMA13* all grew poorly on nonfermentable carbon sources (Ohya et al. 1986, 1991). When examined for defects in mitochondrial respiration, these authors found no decrease in the O_2 consumption rate of intact cells nor defects in mitochondrial F_1-ATPase activity (Ohya et al. 1991). From these data, the conclusion was drawn that mutations in the various *VMA* genes cause no abnormality in mitochondrial function. In our studies, however, we found that intact *vma3* mutants had a reduced rate of O_2 consumption on glycerol and ethanol. Furthermore, we found that O_2 consumption by isolated *vma3* mitochondrial fractions was three- to fourfold lower than the wild-type rate. Although we cannot explain this discrepancy at this time, experiments are currently under way to determine whether strain- or allele-specific differences are responsible.

A striking feature of *vma3* mutants is the ability of iron supplements to suppress their respiratory defect. One explanation for this observation is suggested by recent studies demonstrating that intracellular iron is stored in the vacuole prior to utilization (Raguzzi et al. 1988). An increase in vacuolar pH may reduce the solubility of this stored iron, lower the rate of its transport out of the organelle, and prevent an adequate supply of iron from accumulating in the mitochondria for heme synthesis. This model suggests that *vma3* mutants would have lower levels of cytochromes than wild-type cells yet we found no cytochrome deficiency in *vma3* mutant cells. It is possible that the rate of heme synthesis rather than its absolute level in the cell limits the growth rate of these mutants. Therefore, *vma3* mutants may grow more slowly on respired carbon sources yet still maintain a normal cytochrome level. A link between heme synthesis and the Gef^- phenotype is supported by our recent observation that a *hem1* strain also shows an iron-suppressible petite phenotype (D.E., unpublished observation). *HEM1* encodes δ-aminolevulinic acid (ALA) synthase, which catalyzes the first committed step of the heme biosynthetic pathway (Arrese et al. 1983). Mutants defective in the *HEM1* gene grew poorly on YPGE + 50 μg/ml ALA but grew at a wild-type rate when this medium was supplemented with 5 mM $FeCl_3$. Therefore, we suggest that the respiration defect in *vma3* mutants may in fact be the result of a reduced rate of heme synthesis. This hypothesis has not yet been tested.

Noumi et al. (1991) generated several amino acid substitution mutations in the *VMA3* gene and tested their function in vivo. They identified many residues essential for function of the proteolipid subunit. We have characterized three new mutant alleles of the *VMA3* gene that alter the amino acids at positions not included in their analysis. The residues altered in *gef2-1, gef2-2* and *cup5* are highly conserved, either identical or substituted in a conservative fashion (Dayhoff et al. 1978), among several sequenced vacuolar H^+-ATPase proteolipid subunit genes. These genes were from mammals (Mandel et al. 1988), insects (Meagher et al. 1990), plants (Lai et al. 1991), and an additional *S. cerevisiae* gene found to encode a proteolipid-like protein product, *VMA11* (Umemoto et al. 1991). The protein product of these genes contains four potential transmembrane domains designated I, II, III, and IV. The *gef2-1, cup5,* and *gef2-2* alleles alter the identity of an amino acid in domains I, III, and IV, respectively. The proline to leucine substitution at amino acid 10 in *gef2-1* is a nonconservative alteration and likely to have major effects on protein structure in domain I. Glycine 112 to aspartic acid (*cup5*) is a conservative substitution in many proteins but very disruptive to *VMA3* function. This fact, coupled with the extreme conservation observed at this position (it is invariant in all proteolipid subunit gene sequences published to date), indicates a strong dependence on this glycine residue. Surprisingly, the conservative substitution of alanine-147 with valine (*gef2-2*) also had a profound effect on the function of this protein. This substitution produced a phenotype almost indistinguishable from a mutation in which the gene had been disrupted by insertion of the *LEU2* gene in the middle of the coding region. These observations suggest that the size of the residue side chain at this position is very important for the function of the protein. A similar size dependence was also observed at three nearby positions within transmembrane domain IV, i.e. tyrosine 142, isoleucine 132, and leucine 133 (Noumi et al. 1991). These observations may be indicative of a very close contact between transmembrane domain IV and another protein domain, either within the proteolipid or in another subunit. While the identity of the altered amino acids tells us little about the nature of the defect caused by each mutant allele, the recessive nature of the alleles tested indicated that each can be described as a loss-of-function, or "hypomorphic", allele.

Acknowledgements. We thank Wil Salo and Margaret Broderius for synthesis of oligonucleotides and Ann Thering and Dennis Winge for critical reading of the manuscript. This work was supported by grant GM48139 from the National Institutes of Health.

References

Anraku Y, Ohya Y, Iida H (1991) Cell cycle control by calcium and calmodulin in *Saccharomyces cerevisiae*. Biochim Biophys Acta 1093:169–177

Arrese M, Carvajal E, Robison S, Sambunaris A, Panek A, Mattoon J (1983) Cloning of the δ-aminolevulinic acid synthase structural gene in yeast. Curr Genet 7:175–183

Borson ND, Salo WL, Drewes LR (1992) A lock-docking oligo(dT) primer for 5′- and 3′-RACE PCR. PCR Methods Appl 2:144–148

Bowman EJ, Mandala S, Taiz L, Bowman BJ (1986) Structural studies of the vacuolar membrane ATPase from *Neurospora crassa* and comparison with the tonoplast membrane ATPase from *Zea mays*. Proc Natl Acad Sci USA 83:48–52

Bradford MM (1976) A rapid and sensitive method for the quantitation of microgram quantities of protein utilizing the principle of protein-dye binding. Anal Biochem 72:248–254

Carle GF, Olson MV (1985) An electrophoretic karyotype for yeast. Proc Natl Acad Sci USA 82:3756–3760

Carlson M, Botstein D (1982) Two differentially regulated mRNAs with different 5′ ends encode secreted and intracellular forms of yeast invertase. Cell 28:145–154

Chappell JB (1964) The oxidation of citrate, isocitrate, and cis-aconitate by isolated mitochondria. Biochem J 90:225–237

Dayhoff MO, Schwartz RM, Orcutt BC (1978) A model of evolutionary change in proteins. In: Atlas of protein sequence and structure. National Biomedical Research Foundation, Silver Spring, Md., pp 345–352

Ecker DJ, Butt TR, Sternberg EJ, Neeper MP, Debouck C, Gorman JA, Crooke ST (1986) Yeast metallothionein function in metal ion detoxification. J Biol Chem 261:16895–16900

Gadd GM, White C (1989) Heavy metal and radionuclide accumulation and toxicity in fungi and yeasts. In: Poole RK, Gadd GM (ed) Metal-microbe interactions. IRL Press, Oxford, pp 19–38

Greene JR, Brown NH, Didomenico BJ, Kaplan J, Eide DJ (1993) The *GEF1* gene of *Saccharomyces cerevisiae* encodes an integral membrane protein with mutant effects on respiration and iron-limited growth. Mol Gen Genet, manuscript submitted

Halliwell B, Gutteridge JMC (1992) Biologically relevant metal ion-dependent hydroxyl radical generation. FEBS Lett 307:108–112

Henikoff S (1984) Unidirectional digestion with exonuclease III creates targeted breakpoints for DNA sequencing. Gene 28:351–359

Hill JE, Myers AM, Koerner TJ, Tzagoloff A (1986) Yeast/*E. coli* shuttle vectors with multiple unique restriction sites. Yeast 2:163–167

Kane PM, Yamashiro CT, Stevens TH (1989) Biochemical characterization of the yeast vacuolar H^+-ATPase. J Biol Chem 264:19236–19244

Klionsky DJ, Herman PK, Emr SD (1990) The fungal vacuole: composition, function, and biogenesis. Microbiol Rev 54:266–292

Lagunas R (1986) Misconceptions about the energy metabolism of *Saccharomyces cerevisiae*. Yeast 2:221–228

Lai S, Watson JC, Hansen JN, Sze H (1991) Molecular cloning and sequencing of cDNAs encoding the proteolipid subunit of the vacuolar H^+-ATPase from a higher plant. J Biol Chem 266:16078–16084

Levin DE, Fields FO, Kunisawa R, Bishop JM, Thorner J (1990) A candidate protein kinase C gene, *PKC1*, is required for the *S. cerevisiae* cell cycle. Cell 62:213–224

Mandel M, Moriyama Y, Hulmes JD, Pan YC, Nelson H, Nelson N (1988) cDNA sequence encoding the 16-kDa proteolipid of chromaffin granules implies gene duplication in the evolution of H^+-ATPases. Proc Natl Acad Sci USA 85:5521–5524

Meagher L, McLean P, Finbow ME (1990) Sequence of a cDNA from *Drosophila* coding the 16kD proteolipid component of the vacuolar H^+-ATPase. Nucleic Acids Res 18:6712

Mortimer RK, Schild D (1981) Genetic mapping in *Saccharomyces cerevisiae*. In: Strathern JN, Jones EW, Broach JR (eds) The molecular biology of the yeast *Saccharomyces*: life cycle and inheritance. Cold Spring Harbor Laboratory Press, Cold Spring Harbor, NY, pp 11–26

Nelson H, Nelson N (1989) The progenitor of ATP synthases was closely related to the current vacuolar H^+-ATPase. FEBS Lett 247:147–153

Nelson H, Nelson N (1990) Disruption of genes encoding subunits of yeast vacuolar H^+-ATPase causes conditional lethality. Proc Natl Acad Sci USA 87:3503–3507

Noumi T, Beltran C, Nelson H, Nelson N (1991) Mutational analysis of yeast vacuolar H^+-ATPase. Proc Natl Acad Sci USA 88:1938–1942

Ohsumi Y, Anraku Y (1983) Calcium transport driven by a proton motive force in vacuolar membrane vesicles of *Saccharomyces cerevisiae*. J Biol Chem 258:5614–5617

Ohya Y, Anraku Y (1989) A galactose-dependent *cmd1* mutant of *Saccharomyces cerevisiae*: involvement of calmodulin in nuclear division. Curr Genet 15:113–120

Ohya Y, Ohsumi Y, Anraku Y (1986) Isolation and characterization of Ca^{2+}-sensitive mutants of *Saccharomyces cerevisiae*. J Gen Microbiol 132:979–988

Ohya Y, Umemoto N, Tanida I, Ohta A, Iida H, Anraku Y (1991) Calcium-sensitive *cls* mutants of *Saccharomyces cerevisiae* showing a pet$^-$- phenotype are ascribable to defects of vacuolar membrane H^+-ATPase activity. J Biol Chem 266:13971–13977

Okorokov LA, Kulakovskaya TV, Lichko LP, Polorotova EV (1985) H^+/ion antiport as the principal mechanism of transport systems in the vacuolar membrane of the yeast *Saccharomyces carlsbergensis*. FEBS Lett 192:303–306

Parvin R (1969) Citrate synthase from yeast. Methods Enzymol 13:16–19

Preston RA, Murphy RF, Jones EW (1989) Assay of vacuolar pH in yeast and identification of acidification-defective mutants. Proc Natl Acad Sci USA 86:7027–7031

Raguzzi F, Lesuisse E, Crichton RR (1988) Iron storage in *Saccharomyces cerevisiae*. FEBS Lett 231:253–258

Roberts CJ, Raymond CK, Yamashiro CT, Stevens TH (1991) Methods for studying the yeast vacuole. Methods Enzymol 194:644–661

Rothstein R (1991) Targeting, disruption, replacement, and allele rescue: integrative DNA transformation in yeast. Methods Enzymol 194:281–301

Sambrook J, Fritsch EF, Maniatis T (1989) Molecular cloning: a laboratory manual. Cold Spring Harbor Laboratory Press, Cold Spring Harbor, NY

Sherman F, Fink GR, Hicks JB (1986) Methods in yeast genetics. Cold Spring Harbor Laboratory Press, Cold Spring Harbor, NY

Shih CK, Wagner R, Feinstein S, Kanik-Ennulat C, Neff N (1988) A dominant trifluoperazine resistance gene from *Saccharomyces cerevisiae* has homology with F_0F_1 ATP synthase and confers calcium-sensitive growth. Mol Cell Biol 8:3094–3103

Uchido E, Ohsumi Y, Anraku Y (1985) Purification and properties of H^+-translocating, Mg^{2+}-adenosine triphosphatase from vacuolar membranes of *Saccharomyces cerevisiae*. J Biol Chem 260:1090–1095

Umemoto N, Yoshihisa T, Hirata R, Anraku Y (1990) Roles of the *VMA3* gene product, subunit c of the vacuolar membrane H^+-ATPase on vacuolar acidification and protein transport. J Biol Chem 265:18447–18453

Umemoto N, Ohya Y, Anraku Y (1991) *VMA11*, a novel gene that encodes a putative proteolipid, is indispensible for expression of yeast vacuolar membrane H^+-ATPase activity. J Biol Chem 266:24526–24532

Welch J, Fogel S, Buchman C, Karin M (1989) The *CUP2* gene product regulates the expression of the *CUP1* gene, coding for yeast metallothionein. EMBO J 8:255–260

Yaffe MP (1991) Analysis of mitochondrial function and assembly. Methods Enzymol 194:627–643